**International Journal of Hydrological and Environmental for Sustainability**
**Volume 2, Issue 2, 79-87.**
e_ISSN: 2828-5050
https://www.journal.foundae.com/index.php/ijhes

# Identification of the Distribution and Volume of Iron Sand in the Gura Beach Area Using the Wenner-Schlumberger Configuration Geoelectric Method

**Yumarti G B Tjinta**
Departement of Physics,
Universitas Halmahera,
INDONESIA

**Bayu Achil Sadjab***
Departement of Physics,
Universitas Halmahera,
INDONESIA

**Kurnia**
Departement of Physics,
Universitas Halmahera,
INDONESIA

**Harsen Berg Janis**
Departement of Physics,
Universitas Halmahera,
INDONESIA

**Masitah Yusniar**
Departement of Physics,
Universitas Halmahera,
INDONESIA

**Oktosea Buka**
Departement of Physics,
Universitas Halmahera,
INDONESIA

**Steven Iwamoni**
Dinas Lingkungan Hidup,
Kabupaten Halmahera Utara,
INDONESIA

**Adrian Rahmat Nur**
Departement of Physics,
Universitas Halu Oleo,
INDONESIA

***Correspondence: E-mail:** bayu0604@gmail.com

**Article Info**

***Article history:***

Received: April 28, 2023
Revised: June 28, 2023
Accepted: June 30, 2023



**Abstract**

The Naniura NRD300 HF tool has been used in research using the Wenner-Schlumberger configuration geoelectric method to determine the direction of iron sand distribution, the volume of iron sand, and the concentration of iron sand in the Gura beach area. The collected measurement results are then processed by the RES2DINV software into a 2 Dimension (2D) cross-section that shows the distribution values of the subsurface layer as shown by a color image. Once saved in (.xyz) format, the RES2DINV software results are processed in RockWork software to create pseudo-3D cross sections. The RES2DINV software's results show that line 1's resistivity value ranges from 39.6 to 1000 Ωm, whereas line 2's resistivity value ranges from 0.16 to 1.7 Ωm. These findings suggest that line 2 has a lower resistivity value than line 1 does. The volume of iron sand processed by RockWork software is 221,000 cubic meters for linek 2 and 273,000 cubic meters for line 1. The distribution of iron sand deposits in the study region is south to north, based on the volume of iron sand in line 1, which is bigger. A method used to determine the composition of the minerals present in a sample is called X-ray fluorescence (XRF). The results of analyzing the Fe content in line 2 are 55.01%, which is higher when compared to the Fe content in line 1, which is 40.5%.

**Keywords:** iron sand; wenner-schlumberger configuration; res2dinv software; rockwork software; x-ray flourencence

**To cite this article:** Tjinta, Y, G, B., Sadjab, B, A., Kurnia., Janis, H, B., Yusniar, M., Buka, O., Iwamoni, S, and Nur, A, R. (2023). Identification of the Distribution and Volume of Iron Sand in the Gura Beach Area Using the Wenner-Schlumberger Configuration Geoelectric Method. *International Journal of Hydrological and Environmental for Sustainability, 2*(2), 79-87. https://doi.org/10.58524/ijhes.v2i2.253

## INTRODUCTION

Iron sand contains iron particles, where the formation process comes from the weathering of rocks (containing iron minerals) by weather and sea waves, where these rocks are accumulated, washed by sea waves, and deposited along the coast (Sadjab et al., 2020). Sand containing iron particles is characterized by a grayish or blackish color. Based on initial observations on the Gura village beach, there is sand containing iron. The observation results were indicated by the sand sticking to the bar magnet. Iron sand also has many benefits for industry in steel factories as a raw material and magnetic material from which iron ore is extracted (Cescon & Jiang, 2020).

In identifying the distribution and volume of iron sand using the geoelectric method, it is useful to determine subsurface layers based on the electrical properties of rocks. The geoelectric method is also a method that is quite widely used in the world of exploration, one of which is iron sand exploration, where this method considers the earth as a giant resistor. In this method, many electrode configurations are known, among which the Wenner configuration, Schlumberger configuration and Dipole-dipole configuration are often used (Satriani et al., 2012).

The Wenner-Schlumberger configuration is a geoelectric method electrode configuration that is commonly used for mapping and sounding (Jamaluddin & Umar, 2018; Pratiwi et al., 2019). The Wenner-Schlumberger configuration is also a combined method between the Wenner configuration and the Schlumberger configuration. The resistivity mapping method is a resistivity method which aims to study horizontal variations in the resistivity of subsurface layers. Meanwhile, the resistivity sounding method aims to study vertical variations in the resistivity of rocks below the earth's surface.

The Wenner-Schlumberger configuration has the advantage of vertical and horizontal coverage. The advantage of the Wenner configuration is that the accuracy of the voltage reading on the MN electrode is better with relatively large numbers because the MN electrode is relatively close to the AB electrode. Meanwhile, the advantage of the Schlumberger configuration is the ability to detect non-homogeneity of rock layers on the surface, namely by comparing the apparent resistivity values when there is a change in the MN/2 electrode distance (Aizebeokhai & Oyeyemi, 2015).

Using the Wenner-Schlumberger configuration in this research to determine the conditions below the earth's surface horizontally and vertically. Based on the description above, it is necessary to carry out research to identify the distribution and volume of iron sand in the Gura coastal area using the Wenner-Schlumberger configuration geoelectric method.

## Iron Sand

Iron sand is a kind of sand that contains magnetism along the coast. Gray to blackish color of iron sand, fine grained with a size between 75 – 150 microns, density 2-5 gr/cm$^3$, and magnetic degree 6.40 - 27.16%. The formation of iron sand is a process of destruction from weather and surface water, which is then transported and deposited along the coast **(Figure 1)**. The formation of iron sand deposits is determined by several factors, including the original rock, transportation media, breakdown process and place of deposition. Streams of river water, wind, waves and ocean currents are the transport media for iron sand deposits (Sadjab et al., 2020).

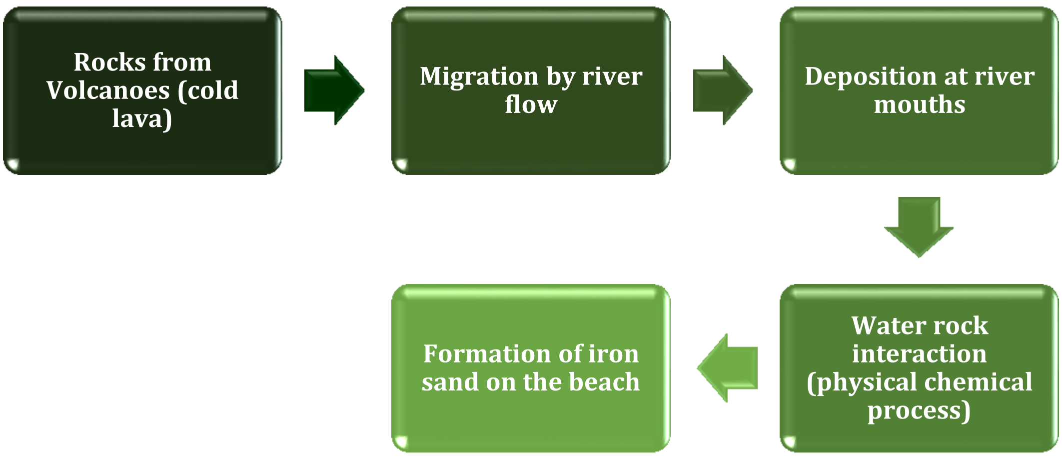


**Figure 1.** Iron sand formation process

Iron sand contains magnetic minerals such as magnetic ($Fe_3O_4$), hematite ($\alpha$-$Fe_2O_3$), maghemite ($\gamma$-$Fe_2O_3$), Magnesium Charomium Oxide (Fe, Mg) $(Cr, Fe)_2O_4$, Spessartine ($Mn_3Al_2Si_3O_{12}$), $SiO_2$/Orthoclase ($KalSi_3O_8$), Spinel ($MgAl_2O_4$), Diamon (C), Marcasite (FeS), Sulfur (S), Chalcopyrite

($CuFeS_2$) / Vanadium (V), and Cuprite ($CuO_2$) (Satria et al., 2021; Tanii et al., 2014; Togibasa et al., 2018).

**Table 1.** Resistivity values in rock and soil materials

| Materials | Resistivity (Ω.m) |
|---|---|
| Bismuth (*Bismuthinite*) | from 18 to 570 |
| Covellite | from $3\times10^{-7}$ to $8\times10^{-5}$ |
| Chalcopyrite | from $1,2\times10^{-5}$ to 0,3 |
| Chalcocite | from $3\times10^{-5}$ to 0,6 |
| Bornite | from $2,5\times10^{-5}$ to 0,5 |
| Pyrite | from $2,9\times10^{-5}$ – 1,5 |
| Pyrrhotite | from $6,5\times10^{-6}$ to $5\times10^{-2}$ |
| Molybdenite | from $10^{-3}$ to $10^{6}$ |
| Galena | from $3\times10^{-5}$ to $3\times10^{2}$ |
| Stanite | from $10^{-3}$ to $10^{6}$ |
| Stibnite | from $10^{5}$ to $10^{12}$ |
| Sphalerite | from 1,5 to $10^{7}$ |
| Cobalt (*Cobaltite*) | from $3,5\times10^{-4}$ to $10^{-1}$ |
| Arsenopyrite | from $2\times10^{-4}$ to $10^{-1}$ |
| Niccolite | from $10^{-7}$ to $2\times10^{-3}$ |
| Bauxite | from $2\times10^{2}$ to $6\times10^{-3}$ |
| Cuprite | from $10^{-3}$ to 300 |
| Chromite | from 1 to $10^{-6}$ |
| Iron ore (*Hematite*) | from $3,5\times10^{-3}$ to $10^{7}$ |
| Limonite | from $10^{3}$ to $10^{7}$ |
| Mangnetite | from $5\times10^{-5}$ to $5,7\times10^{3}$ |
| Ilmenit | from $10^{-3}$ to 50 |
| Wolframite | from 10 to $10^{5}$ |
| Pyrolusite | from $5\times10^{-3}$ to 10 |
| Quartz | from $4\times10^{10}$ to $2\times10^{14}$ |
| Cassirite | from $4\times10^{-4}$ to $10^{4}$ |
| Rutile | from 300 to 1000 |
| Uraninite | from 1 to 200 |
| Rock salt | from 30 to $10^{13}$ |
| Sylvite | from $10^{11}$ to $10^{12}$ |
| Diamond | from 10 to $10^{14}$ |
| Serpentine | from $2\times10^{2}$ to $3\times10^{3}$ |
| Hornblede | from $2\times10^{2}$ to $10^{6}$ |
| Mica | from $9\times10^{2}$ to $10^{14}$ |
| Biotite | from $2\times10^{2}$ to $10^{6}$ |
| Bitum coal | $\pm 0,6\times10^{5}$ |
| Anthracite | from 9 to 200 |
| Lignite | from 30 to $10^{3}$ |
| Groundwater | from 0,5 to 300 |
| Sand | from 1 to $10^{3}$ |
| Sandstone | from 1 to $6,4\times10^{8}$ |
| Tufa | from 20 to 100 |
| Iron Sand | from 0,13 to 2,87 |
| Breccia | from 75 to 200 |

**Sources:** (Telford & W.M. Telford, 2004)

## METHOD

Research on identifying the distribution and volume of iron sand using the Wenner-Schlumberger configuration geoelectric method was carried out on the beach of Gura village, Tobelo District, North Halmahera Regency **(Figure 2)** on Saturday, December 7, 2019. The tools and materials used in the research were a Naniura NRD 300 HF resistivity meter, 2 iron and copper electrodes each, 4 roller cables, a dry battery, one meter, stationery and a camera.

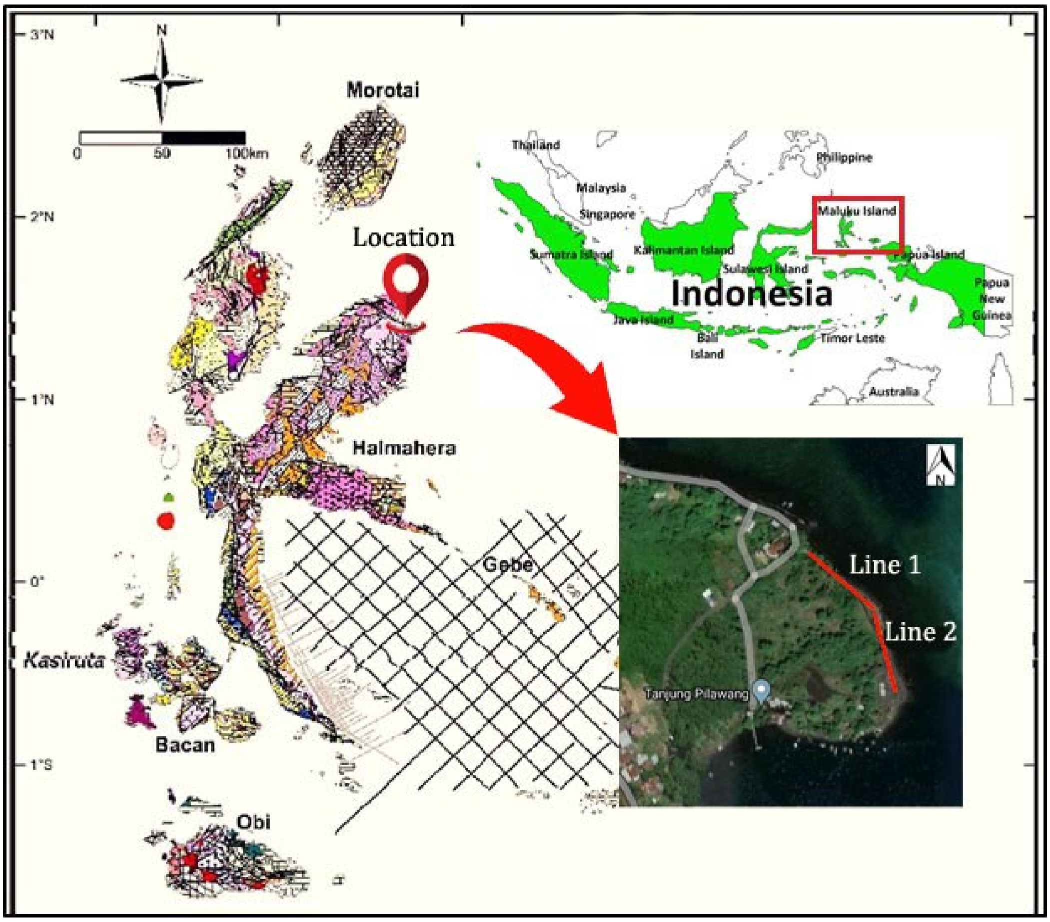


**Figure 2.** Research location map

### Wenner-Schlumberger Configuration

A configuration with a constant spacing rule system with a factor of "n" is a Wenner-Schlumberger configuration. Configuration is the comparison of the distance between AM and MN electrodes. If the distance between the MN electrodes is $a$ then the distance between the current electrodes (A and B) is 2na + $a$. Straight line is the process of determining resistivity on 4 electrodes (Satriani et al., 2012). The geometric factors of the Wenner-Schlumberger configuration are: k = n (n+1) $\pi a$. Where $a$ is the distance between electrodes M and N **(Figure 3)**.

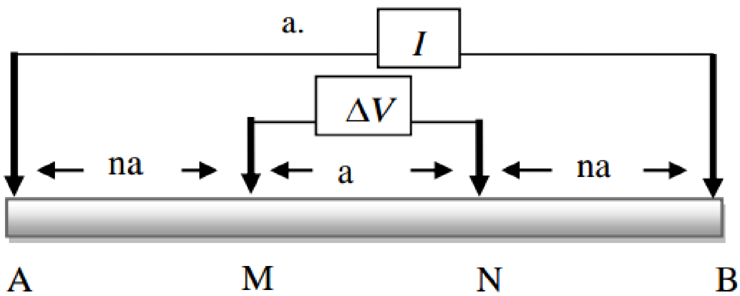


**Figure 3.** Wenner-Schlumberger configuration electrode

### X-Ray Fluorescence

X-Ray Fluorescence (XRF) is a tool used to analyze the composition of the mineral content contained in a sample (Hayashi & Korecki, 2018). XRF has several advantages, including being multi-elemental or being able to detect various kinds of materials, fast analysis and the results are qualitative analysis and quantitative analysis. Qualitative analysis informs the type of element contained in the sample being analyzed which is determined by the element's spectrum in the X-ray characterization, while quantitative analysis informs the number of elements contained in the sample which is determined by the peak height of the spectrum (Pushie et al., 2014).

The working principle of the XRF device is as follows: the fluorescence x-rays emitted by the sample are produced by irradiating the sample with primary x-rays from the x-ray tube, which are generated with electrical energy from a voltage source of 1200 volts. When radiation from an x-ray tube hits a sample, the electrons in the sample will be excited to a lower energy level, emitting characteristic x-rays. These characterization x-rays captured by the detector are converted into a voltage signal, amplified by the preamp and fed into the analyzer for data processing (Chorus & Bartram, 1999; Hayashi & Korecki, 2018; Pushie et al., 2014; Sadjab et al., 2020).

### Data Collection Procedures

The first step taken is a location survey, if the location meets the requirements for conducting research, the next step is for researchers to prepare tools and materials to be used in the field, the tools used are geoelectric resistivity meters and other supporting tools. Install the electrodes and the potential of the Wenner-Schlumberger configuration with a predetermined distance, when taking current source data originating from the battery is injected into the earth through two current electrodes that have been plugged into the earth's surface. The existence of the flow of electric current will cause an electric voltage. The voltage that occurs through the two potential electrodes is measured using a multimeter that is already in the geoelectric resistivity meter.

### Data analysis

Based on the data that has been obtained in the field, it is then processed using the RES2DINV software. RES2DINV software can describe or create 2-dimensional subsurface models from geoelectric survey data. The results obtained from data processing in the RES2DINV software show conditions that are close to the actual subsurface if the inversion results produce very small error values. The smaller the error value obtained, the better the quality of the subsurface cross section based on the existing resistivity data. RockWorks Software is software that helps with this model subsurface conditions so well that it is able to describe subsurface structures in 3D models. RockWorks software provides mining, environmental and petroleum planning.

## RESULTS AND DISCUSSION

### Description of the research location

The research location is located on the coast of Gura Village, the research was carried out in 2 passes, line 1 was at the coordinate point south latitude 1°44'16.494'' east longitude 128°0'39.996'' and line 2 was at the coordinate point south latitude 1°44 '12.576'' east longitude 128°0'43.218'' **(Figure 2)** in this research the line distance is 150 meters each. Physiographically, Halmahera Island is divided into three parts, namely the East Halmahera physiographic area, the West Halmahera physiographic area, and the Quaternary volcanic island arc area **(Figure 4.A)**. The stratigraphy of the study area consists of 11 formations which range in age from before the Jurassic to the Holocene **(Figure 4.B)**.

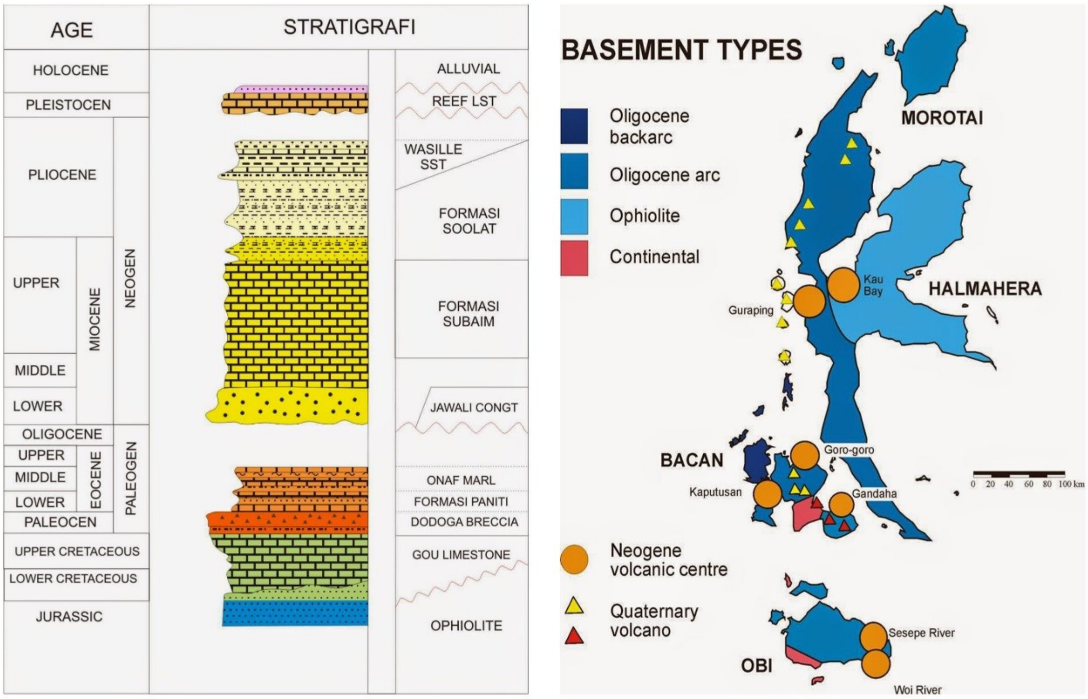


A B

**Figure 4. A.** Geological map of Maluku Island; **B.** Stratigrafi regional Halmahera

## Geoelectric Data Analysis

The data obtained from direct field observations are in the form of current data (I), potential difference data (V), apparent resistivity data (ρ), datum point data, spacing, number of layers. The data obtained was then processed using the RES2DINV software for the two parallel lines along the coast of Gura Village. The processing result of this software is in the form of 2D inversion which can then be saved in (.xyz) format. Data in (.xyz) format consists of accumulated electrode distance, true resistivity value, depth of current penetration, and subsurface conductivity based on measurement results.

In the line1, the resistivity data inversion presented in 2D cross section **(Figure 5)**. Based on **Figure 5**, the Wenner-Schlumberger configuration is capable of measuring subsurface structures up to 25 meters. At a depth of 2.50 – 24.9 meters from the surface the datum point 60 – 230 meters has a resistivity value of 0.57 – 10 Ωm dominated by dark blue and light blue images assumed to be iron sand, while resistivity values are 39.6 –1000 Ωm dominated by green and yellow color images assumed to be sand. The surface of the datum point 25-60 meters has a resistivity value of 3000> Ωm dominated by red image which is assumed to be sandstone. Based on the processing results of the RES2DINV Software, it can be interpreted that below the surface on the beach in Gura village there are several materials including iron sand, sand and sandstone.

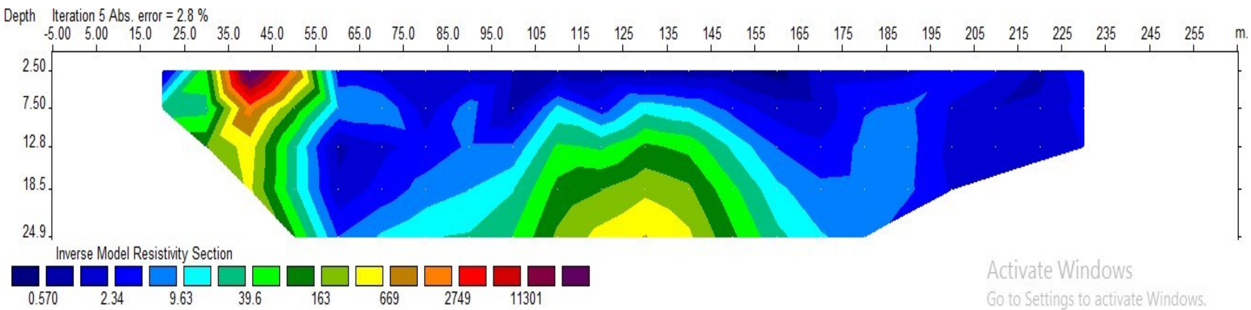


**Figure 5.** 2 Dimension (2D) cross section resistivity contrast of subsurface rocks in line 1

Based on the RES2DINV processing data, it can be seen that the distribution of iron sand deposits in line 1 is spread along the research. The processed data in the form of (.xyz) format was reprocessed using RockWorks software to determine the volume **(Figure 6)**, it can be seen that the distribution of iron sand deposits processed by RockWorks has synchronization with the results shown by the RES2DINV processing results. Based on volume calculations with a resistivity value limit of 0 – 10 Ωm, the volume of iron sand in line 1 is 273,000 $m^3$.

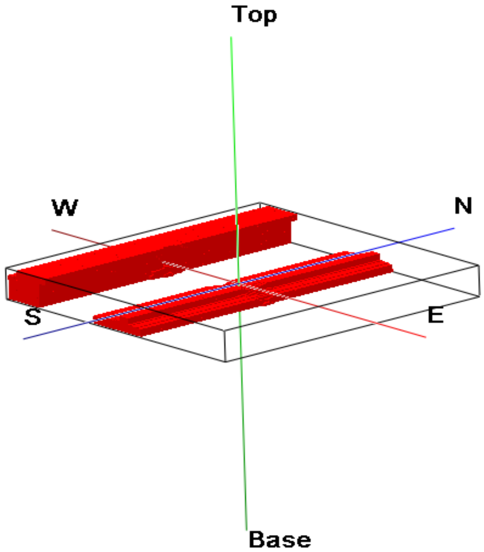


**Figure 6.** Pseudo 3D cross section in line 1

Based on line 2, the inversion results of 2D cross-sectional resistivity data **(Figure 7)**, it can be seen that at a depth of 2.50 – 14 meters it has a resistivity value of 0.16 – 1.7 Ωm with the blue image assumed to be iron sand as in **Table 1** . Depth 18.5 – 24.9 is dominated by green and red color images with resistivity values of 5.38 – 540 Ωm assumed to be sand. Based on the results obtained from the RES2DINV software processing, it can be seen that the materials below the surface are iron sand and sand in **Table 1**.

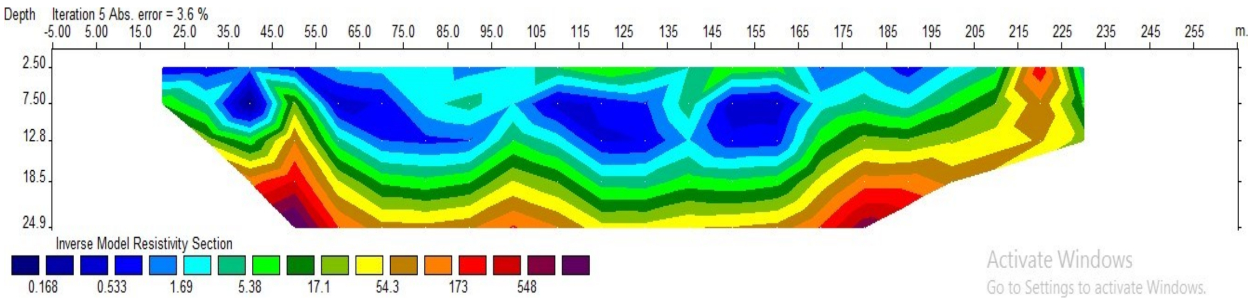


**Figure 7.** 2D cross section resistivity contrast of subsurface rocks in line 2

In the **Figure 7**, 2D Cross-section Resistivity Contrast of Subsurface Rocks line 2. The 3D pseudo-section results of resistivity data based on the results of the RES2DINV inversion **(Figure 8)**. In **Figure 8** the volume of iron sand in the study area is 221,000 $m^3$.

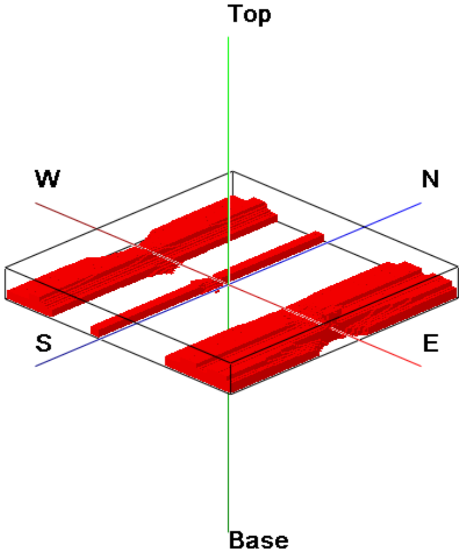


**Figure 8.** Pseudo 3D cross section in line 2

**XRF Analysis of Iron Sand**

In **Table 2** there are several compound compositions in each sand sample at two points, namely $Al_2O_3$ compounds with levels of 6.0% (T1) and 10% (T2), $SiO_2$ compounds with levels of 33.1% (T1) and 42.9 % (T2), $K_2O$ compound with a content of 1.2% (T1) and 2.71% (T2), CaO compound with a content of 10.1% (T1) and 10.9% (T2), $TiO_2$ compound with a content of 3 .36% (T1) and 2.13% (T2), $V_2O_5$ compounds with levels of 0.32% (T1) and 0.15% (T2), $Cr_2O_3$ compounds with levels of 0.085% (T1) and 0.059 (T2), MnO compound 0.59% (T1) and 0.44% (T2), $Fe_2O_3$ compound with a content of 44.2% (T1) and 29.5% (T2), CuO compound with a content of 0.089% (T1) and 0, 10% (T2), ZnO compounds with levels of 0.01% (T1) and 0.02% (T2), $Eu_2O_3$ compounds with levels of 0.50% (T1) and 0.37% (T2) and $Re_2O_7$ compounds with levels 0.30% (T1) and 0.2% (T2).

**Table 2.** Results of analysis of element composition in sand samples

| No | Elements | Composition (%) | |
|---|---|---|---|
| | | **T1** | **T2** |
| 1 | Al | 7,7 | 4,5 |
| 2 | Si | 30,0 | 22,1 |
| 3 | K | 3,71 | 1,56 |
| 4 | Ca | 13,4 | 11,3 |
| 5 | Ti | 2,25 | 3,22 |
| 6 | V | 0,19 | 0,35 |
| 7 | Cr | 0,070 | 0,092 |
| 8 | Mn | 0,68 | 0,81 |
| 9 | Fe | 40,5 | 55,01 |
| 10 | Cu | 0,17 | 0,13 |
| 11 | Zn | 0,04 | 0,02 |
| 12 | Eu | 0,46 | 0,57 |
| 13 | Re | 0,3 | 0,40 |

**Note:** T1 (point 1); T2 (point 2).

## CONCLUSION

The results of research on identifying the distribution and volume of iron sand in the coastal area of Gura village using the Wenner-Schlamberger configuration resistivity geoelectric method, can be concluded that the resistivity value on path 1 is 39.6 – 1000 Ωm, while on path 2 the resistivity value is 0.16 – 1.7 Ωm. From these results it can be assumed that path 2 has a lower resistivity value compared to path 1, so the lower the resistivity value (ability to inhibit electric current) in the material, the higher the conductivity value (ability to conduct electric current) in the material. Based on the volume of iron sand in line 1, it is larger so that the distribution pattern of iron sand deposits is directed from south to north in the study area. The volume of iron sand on line 1 is 273,000 cubic meters, while on line 2 it is 221,000 cubic meters. The Fe element content in path 2 is 55.01%, which is higher than the Fe content in path 1, which is 40.5%.

## CONFLICTS OF INTEREST

The authors declare no conflict of interest concerning the publication of this article. The authors also confirm that the data and the article are free of plagiarism.

## REFERENCES

Aizebeokhai, A. P., & Oyeyemi, K. D. (2015). Application of geoelectrical resistivity imaging and VLF-EM for subsurface characterization in a sedimentary terrain, Southwestern Nigeria. *Arabian Journal of Geosciences*, *8*(6), 4083–4099. https://doi.org/10.1007/s12517-014-1482-z

Cescon, A., & Jiang, J. Q. (2020). Filtration process and alternative filter media material in water treatment. *Water (Switzerland)*, *12*(12), 1–20. https://doi.org/10.3390/w12123377

Chorus, I., & Bartram, J. (1999). Toxic Cyanobacteria in Water: A guide to their public health consequences, monitoring and management. In *Cytometry Part A* (Vol. 95, Issue 8). E & FN Spon, an imprint of Routledge. https://doi.org/10.1002/cyto.a.23870

Hayashi, K., & Korecki, P. (2018). *X-ray Fluorescence Holography : Principles , Apparatus , and Applications d ± H. 061003*, 1–11. https://doi.org/10.7566/JPSJ.87.061003

Jamaluddin, & Umar, E. P. (2018). Identification of subsurface layer with Wenner-Schlumberger arrays configuration geoelectrical method. *IOP Conference Series: Earth and Environmental Science*, *118*(1). https://doi.org/10.1088/1755-1315/118/1/012006

Pratiwi, E. S., Sartohadi, J., & Wahyudi. (2019). Geoelectrical Prediction for Sliding Plane Layers of Rotational Landslide at the Volcanic Transitional Landscapes in Indonesia. *IOP Conference Series: Earth and Environmental Science*, *286*(1). https://doi.org/10.1088/1755-1315/286/1/012028

Pushie, M. J., Pickering, I. J., Korbas, M., Hackett, M. J., & George, G. N. (2014). *Elemental and Chemically Speci fi c X ‑ ray Fluorescence Imaging of Biological Systems*.

Sadjab, B. A., Indrayana, I. P. T., Iwamony, S., & Umam, R. (2020). Investigation of The Distribution and Fe Content of Iron Sand at Wari Ino Beach Tobelo Using Resistivity Method with Werner-Schlumberger Configuration. *Jurnal Ilmiah Pendidikan Fisika Al-Biruni*, *9*(1), 141–160. https://doi.org/10.24042/jipfalbiruni.v9i1.5394

Satria, B., Masrurah, Z., & Fajar, S. J. (2021). Heliyon Magnetic susceptibility and grain size distribution as prospective tools for selective exploration and provenance study of iron sand deposits : A case study from Aceh , Indonesia. *Heliyon*, *7*(March 2020), e08584. https://doi.org/10.1016/j.heliyon.2021.e08584

Satriani, A., Loperte, A., Imbrenda, V., & Lapenna, V. (2012). Geoelectrical surveys for characterization of the coastal saltwater intrusion in metapontum forest reserve (Southern Italy). *International Journal of Geophysics*, *2012*. https://doi.org/10.1155/2012/238478

Tanii, H., Inazumi, T., & Terashima, K. (2014). *Mineralogical Study of Iron Sand with Different Metallurgical Characteristic to Smelting with Use of Japanese Classic Iron- making Furnace " Tatara ." 54*(5), 1044–1050.

Telford, W. M., & W.M. Telford, L. P. G. and R. E. S. (2004). *Applied Geophysics* (Second). Press Syndicate of the Univesity of Cambridge.

Togibasa, O., Bijaksana, S., & Novala, G. C. (2018). *Magnetic Properties of Iron Sand from the Tor River*. 1–7. https://doi.org/10.3390/geosciences8040113